JOC Featured Article

pubs.acs.org/joc

Solvent Effects on Photoreactivity of Valerophenone: A Combined QM and MM Study

Lina Ding, Lin Shen, Xue-Bo Chen, and Wei-Hai Fang*

College of Chemistry, Beijing Normal University, Beijing 100875, China

fangwh@bnu.edu.cn

Received September 26, 2009

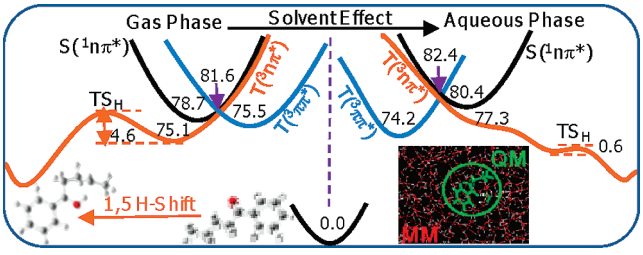

Norrish type reactions for valerophenone in aqueous solution have been investigated by using the combined methods of DFT, CASSCF, and CASPT2 with molecular mechanics. It was found that formation of the intermolecular hydrogen bond in the complex of valerophenone with water results in a blue shift of the n,π^* excited states, while the Coulomb interaction between valerophenone and the bulk surrounding water is mainly responsible for the red shift of the π,π^* excited states. As a result, the $^3\pi\pi^*$ state becomes the lowest triplet state and is responsible for the long triplet lifetime observed for aqueous valerophenone. The $^1n\pi^*$, $^3\pi\pi^*$, and $^3n\pi^*$ states were found to intersect in the same structural region, which appears to be the main reason why the intersystem crossing from $^1n\pi^*$ to $^3n\pi^*$ is very efficient for aqueous valerophenone and why most aromatic ketones have unique photophysical features such as a short singlet lifetime, high phosphorescence, and weak fluorescence. The Coulomb interaction between valerophenone and the bulk surrounding water has a significant influence on the α-C−C cleavage and the 1,5-H shift reaction. The 1,5-H shift is predicted to have a very small barrier on the triplet pathway and the α-C−C bond cleavages are not in competition with the 1,5-H shift reaction. This is in good agreement with the experimental findings that Norrish type II quantum yield is close to unity upon photoexcitation of aqueous valerophenone in the wavelength region of 290−330 nm.

Introduction

Mechanistic photochemistry of a polyatomic molecule has long been regarded as an intellectually challenging area, the results of which are relevant to atmospheric chemistry,[1−3] biological systems,[4−6] and other fields.[7−11] It has been well-established that compounds containing carbonyl groups play an important role in the development of our understanding of photochemistry and photophysics of polyatomic molecules.[12] Photodissociation of carbonyl compound has served as the basis for developing new experimental techniques for direct observation of transient intermediate[13,14]

(1) Donaldson, D. J.; Tuck, A. F; Vaida, V. *Chem. Rev.* **2003**, *103*, 4717–4729.
(2) Matsumi, Y.; Kawasaki, M. *Chem. Rev.* **2003**, *103*, 4767–4781.
(3) Cohen, R. C.; Murphy, J. G. *Chem. Rev.* **2003**, *103*, 4985–4998.
(4) Crespo-Hernandez, C. E.; Cohen, B.; Hare, P. M.; Kohler, B. *Chem. Rev.* **2004**, *104*, 1977–2019.
(5) Lee, I.-R.; Lee, W.; Zewail, A. H. *Proc. Natl. Acad. Sci. U.S.A.* **2006**, *103*, 258–262.
(6) Sinicropi, A.; Andruniow, T.; Ferre, N.; Basosi, R.; Olivucci, M. *J. Am. Chem. Soc.* **2005**, *127*, 11534–11535.
(7) Mitschke, U.; BaEuerle, P. *J. Mater. Chem.* **2000**, *10*, 1471–1507.
(8) Adachi, S.-I.; Park, S.-Y.; Tame, J. R. H.; Shiro, Y.; Shibayama, N. *Proc. Natl. Acad. Sci. U.S.A.* **2003**, *100*, 7039–704.
(9) Heintz, O.; Robert, D.; Weber, J. V. *J. Photochem. Photobiol. A* **2000**, *135*, 77–80.
(10) Zwiener, C; Glauner, T; Frimmel, F. H. *Water Supply* **2003**, *3*, 321–329.
(11) Fujioka, K.; Shibamoto, T. *Environ. Toxicol.* **2006**, *21*, 47–55.
(12) Maciejewski, A.; Steer, R. P. *Chem. Rev.* **1993**, *93*, 67–98. and references therein.
(13) Srinivasan, R.; Feenstra, J. S.; Park, S. T.; Xu, S. J.; Zewail, A. H. *Science* **2005**, *307*, 558–563.
(14) Park, S. T.; Feenstra, J. S; Zewail, A. H. *J. Chem. Phys.* **2006**, *124*, 174707.

Published on Web 11/04/2009 DOI: 10.1021/jo902080z

and for discovering new mechanisms of photochemical reactions.[15−20] Irradiation of a carbonyl compound from the ground state (S_0) to its excited state may lead to cleavage of a bond α to the carbonyl group, which is known as Norrish type I reaction. When γ-hydrogen was included in a carbonyl compound, the 1,5-hydrogen shifts (Norrish type II reaction) could also take place, yielding a 1,4-biradical. The mechanistic details and the related dynamics of these Norrish type reactions are essential to understanding the photochemistry of carbonyl compounds.

Because of the conjugation interaction between the aromatic ring and the carbonyl group, aromatic alkyl ketones exhibit some unique photophysical and photochemical properties, which have been the subject of numerous experimental investigations over the past several decades.[21−41] It was well-established that the first singlet excited state (S_1) lifetime for aromatic ketones (ArCOR) is much shorter than that for aliphatic ketones in the gas and condensed phases. Aromatic carbonyl compounds are highly phosphorescent but only weakly fluorescent. Both singlet and triplet n,π* states can undergo Norrish type I and II reactions for aliphatic ketones. However, for most aromatic ketones or aldehydes, the Norrish type reactions only occur in the triplet state.

Wagner et al. have carried out extensive studies[21−28] on conformational and substituent effects on photoreactivity of aromatic ketones. They pointed out that phenyl alkyl ketones generally undergo Norrish type reactions from their ^{3}nπ* states, while the ketone triplets that are mostly π,π* in character display greatly reduced reactivity in hydrogen abstraction reactions. It was found that various substituents at *o*-, *p*-, or *m*-position of the aromatic ring can have an important influence on the nature of the lowest triplet state. Both electron-donating and electron-withdrawing substituents at the aromatic ring were found to reduce type II quantum yields. The β- and γ-alkyl substitutions were not observed to have steric hindrance to γ-hydrogen abstraction, but rates of the abstraction by triplet states of phenyl alkyl ketones were significantly increased, due to β- and γ-alkyl substitutions. The α-alkyl substitution can produce benzoylcyclopropane with a reasonable yield upon n→π* excitation.[29] Valerophenone was confirmed to show a dramatic shift of photoreactivity by a cyclopropyl group at the α-position to the carbonyl group.[30]

It was shown that the kinetics and the product distribution may be altered significantly by medium properties.[31−41] High dielectric and polar solvents affect the relative energies of the ^{3}nπ* and ^{3}ππ* excited states. The H-bond interaction between solvent and the solute has a noticeable influence on the subsequent reactions of the biradical intermediate. The photoreactivity of valerophenone was investigated as a function of temperature, pH, and wavelength in aqueous solution.[34] Norrish type II quantum yields for the photoreaction of valerophenone were observed to be close to unity throughout the 290−330 nm spectral region and in the temperature range from 10 to 40 °C. On the basis of quenching studies with steady-state irradiations, the triplet lifetime of valerophenone at 20 °C was estimated to be 52 ns, ∼7 times longer than that observed in hydrocarbon solvents, which indicates that the rate constant for γ-hydrogen abstraction is significantly lowered in aqueous media.

Investigations on the photochemistry of aromatic ketones adsorbed on solid surfaces or in solid solutions have attracted a great deal of attention in heterogeneous photochemistry and/or surface photochemistry.[35−41] Photochemical efficiency was found to be independent of the solid solvents used, which can prevent drastic conformational, translational, and rotational changes along the reaction coordinate. However, the α-C−C bond cleavage of valerophenone was not observed due to physical restraints of the solid solvent cavity.[38−41]

Experimental investigations on the photoreactions of aromatic alkyl ketones over the past several decades have provided a wealth of information concerning medium effects on the reactivity. However, a detailed understanding of mechanistic photochemistry of any system must be based on experimental measurements and theoretical calculations on structures and reactivity of the ground and excited electronic states.[12] To our knowledge, there are only three reports that involve ab initio studies on the mechanistic photochemistry of aromatic carbonyl compounds in the gas phase,[42−44] and solvent effects on photoreactivity of aromatic alkyl ketones have not been investigated from a theoretical perspective up to date. Here we report the first theoretical study on Norrish type I and II reactions of

(15) Feenstra, J. S; Park, S. T.; Zewail, A. H. *J. Chem. Phys.* **2005**, *123*, 221104.
(16) Townsend, D.; Lahankar, S. A.; Lee, S. K.; Chambreau, S. D.; Suits, A. G.; Zhang, X.; Rheinecker, J.; Harding, L. B.; Bowman, J. M. *Science* **2004**, *306*, 1158–1161.
(17) Yin, H. M.; Kable, S. H.; Zhang, X.; Bowman, J. M. *Science* **2006**, *311*, 1443–1446.
(18) Houston, P. L.; Kable, S. H. *Proc. Natl. Acad. Sci. U.S.A.* **2006**, *103*, 16079–16082.
(19) Suits, A. G. *Acc. Chem. Res.* **2008**, *41*, 873–881. and references therein.
(20) Fang, W. H. *Acc. Chem. Res.* **2008**, *41*, 452–457.
(21) Wagner, P. J.; Kemppainen, A. E.; Schott, H. N. *J. Am. Chem. Soc.* **1970**, *92*, 5280.
(22) Wagner, P. J. *Acc. Chem. Res.* **1971**, *4*, 168–177.
(23) Wagner, P. J.; Kelso, P. A.; Zepp, R. G. *J. Am. Chem. Soc.* **1972**, *94*, 7480–7488.
(24) Wagner, P. J.; Kemppainen, A. E. *J. Am. Chem. Soc.* **1972**, *94*, 7495–7499.
(25) Wagner, P. J.; Kelso, P. A.; Kemppainen, A. E.; Zepp, R. G. *J. Am. Chem. Soc.* **1972**, *94*, 7500–7506.
(26) Wagner, P. J.; Kemppainen, A. E.; Schott, H. N. *J. Am. Chem. Soc.* **1973**, *95*, 5604–5614.
(27) Wagner, P. J. *Acc. Chem. Res.* **1983**, *16*, 461–467.
(28) Wagner, P. J. *Acc. Chem. Res.* **1989**, *22*, 83–91.
(29) Wessig, P.; Muhling, O. *Angew. Chem., Int. Ed.* **2001**, *40*, 1064–1065.
(30) Park, B. S.; Cho, S.; Chong, S. H. *Bull. Korean Chem. Soc.* **2007**, *28*, 1156–1158.
(31) Ariel, S.; Ramamurthy, V.; Scheffer, J. R.; Trotter, J. *J. Am. Chem. Soc.* **1983**, *105*, 6959.
(32) Evans, S.; Omkaram, N.; Scheffer, J. R. *Tetrahedron Lett.* **1985**, *26*, 5903.
(33) Warren, J. A.; Bernstein, E. R. *J. Chem. Phys.* **1986**, *85*, 2365–2367.
(34) Zepp, R. G.; Gumz, M. M.; Miller, W. L.; Gao, H. *J. Phys. Chem. A* **1998**, *102*, 5716–5723.
(35) Weiss, R. G.; Ramamurthy, V.; Hammond, G. S. *Acc. Chem. Res.* **1993**, *26*, 530–538.
(36) Ihmels, H.; Scheffer, J. R. *Tetrahedron* **1999**, *55*, 885.
(37) Hasegawa, T.; Kajiyama, M.; Yamazaki, Y. *J. Phys. Org. Chem.* **2000**, *13*, 437–442.
(38) Klan, P.; Janosek, J.; Kirz, Z. *J. Photochem. Photobiol. A* **2000**, *134*, 37–44.
(39) Litersk, J.; Klan, P.; Heger, D.; Loupy, A. *J. Photochem. Photobiol. A* **2003**, *154*, 155–159.
(40) Muller, P.; Loupy, A.; Klan, P. *J. Photochem. Photobiol. A* **2005**, *172*, 146–150.
(41) Annalakshmi, S.; Pitchumani, K. *Bull. Chem. Soc. Jpn.* **2005**, *78*, 2000–2006.
(42) Fang, W.-H.; Phillips, D. L. *Chem. Phys. Chem.* **2002**, *3*, 889–892.
(43) Fang, W.-H.; Phillips, D. L. *J. Theor. Comput. Chem.* **2003**, *2*, 23–31.
(44) He, H.-Y.; Fang, W.-H.; Phillips, D. L. *J. Phys. Chem. A* **2004**, *108*, 5386–5392.

valerophenone in aqueous solution using combined molecular mechanics (MM) and high-level ab initio methods (QM). Structures and relative energies of the lowest five electronic states were determined for valerophenone in aqueous solution. The three potential energy surfaces were found to intersect in the Franck−Condon region, which gives a reasonable explanation why the intersystem crossing (ISC) to the triplet state is so efficient for aromatic ketones in aqueous solution. The mechanistic details for photoreaction of valerophenone in aqueous solution are characterized in the present study. We believe that the results reported here provide new insights into the interesting and complex photochemistry of aromatic carbonyl compounds in aqueous solution.

Computational Methods

To mimic the dynamic nature of valerophenone (VP) in the water environment, we built a water box of $32 \times 27 \times 27$ Å^3 with the VP enclosed and then ran a 15 ns molecular dynamics (MD) simulation. A few snapshots, which exhibit relatively high stability in the MD simulation time range (5−15 ns), were employed as the starting geometries for the combined quantum mechanics (QM) and molecular mechanics (MM) calculations. The complex of valerophenone with one H_2O molecule (VP−H_2O) was found to be formed with high probability in the MD simulation. Therefore, the VP−H_2O complex is treated as the QM subsystem. The remaining H_2O molecules are calculated at the molecular mechanical level utilizing the Amber force field via iterative QM and MM optimizations. The total energy of the QM/MM system can be written as follows

$$E = E_{\mathrm{QM}} + E_{\mathrm{MM}} + E_{\mathrm{QM/MM}} \quad (1)$$

where E_{QM} is the quantum mechanical energy of the QM subsystem, and E_{MM} is the standard molecular mechanical interactions involving exclusively atoms in the MM subsystem. Since there is no covalent bond interaction between the QM and MM subsystems, the QM/MM interaction includes mainly the electrostatic and the van der Waals contributions

$$E_{\mathrm{QM/MM}} = E_{\mathrm{electrostatic}}(\mathrm{QM/MM}) + E_{\mathrm{vdW}}(\mathrm{QM/MM}) \quad (2)$$

For electrostatic interactions, we first fit the electrostatic potential from the QM calculations and obtained the effective charge on each QM atom. Then we calculated the Coulomb interactions between the point charges of the QM atoms and the point charges of MM atoms

$$\left\langle \Psi \left| -\sum_{i}^{N} \sum_{\beta \in \mathrm{MM}} \frac{q_\beta}{r_{\beta i}} + \sum_{\alpha \in \mathrm{QM}, \beta \in \mathrm{MM}} \frac{Z_\alpha q_\beta}{r_{\alpha\beta}} \right| \Psi \right\rangle = \sum_{\alpha \in \mathrm{QM}, \beta \in \mathrm{MM}} \frac{Q_\alpha q_\beta}{r_{\alpha\beta}} \quad (3)$$

where N is the total number of electrons of each QM atom, Z_α is the charge of the nuclei of QM atom, q_β is the point charge of MM atom from the Amber 94 force field, and Q_α is the electrostatic potential fitted point charge of QM atom. In addition, the Amber force field parameters were used to calculate the van der Waals contributions, which is very small in comparison with the Coulomb interaction.

Three different methods were used for the QM calculations. Hybrid density functional theory (DFT) with the B3LYP exchange-correction functional is able to treat rather large systems in the ground and lowest triplet states, and the calculated results reproduced experimental structures and energies with good accuracy. The B3LYP/6-311G** method was first used to optimize the stationary structures in the ground and triplet states. The complete active space self-consistent field (CASSCF) wave function has sufficient flexibility to model the changes in electronic structure upon electronic excitation. The CASSCF calculations were performed for valerophenone and its one-water complex in the lowest five electronic states (S_0, S_1, T_1, S_2, and T_2), which provide a balanced description of the minimum energy structures of the lowest five electronic states. To refine the relative energies of the stationary structures in different electronic states, the single-point energy is calculated with the multiconfigurational perturbation method (CASPT2) on the CASSCF reference wave functions. The CASPT2 energies are calculated using five-root state-averaging with equal weights. The 6-31G* basis set, which has been confirmed to be reliable in previous studies,[42−44] is chosen for the CASSCF and CASPT2 calculations. Ten electrons distributed in nine orbitals are included in the active space for the CASSCF calculation, referred to as CAS(10,9) hereafter, which originate from the three π and three π^* orbitals in the aromatic ring, the C−O π and π^* orbitals, and the oxygen nonbonding orbital.

An iterative QM and MM optimization procedure[45,46] was used to determine stationary structures of the one-water complex in aqueous solution. Structure of the QM subsystem was first optimized at the B3LYP/6-311G** or CAS(10,9)/6-31G* level with the fixed structure for the MM subsystem fixed. Once convergence is reached, the electrostatic potential is fitted to obtain the effective charge on each QM atom. Then, the geometric structure of the MM subsystem was optimized at the MM level with the QM subsystem fixed at the B3LYP/6-311G** or CAS(10,9)/6-31G* optimized bond parameters. The previous steps are repeated until the maximum force and its root-mean-square are less than 0.00045 and 0.0003 hartree/bohr, respectively. The combined CAS(10,9)/Amber and B3LYP/Amber calculations are performed by the Gaussian 03 program[47] package that linked to the Gromacs and Tinker tool package, while the CASPT2//CASSCF/Amber calculations are performed by the Molcas[48] linked to Tinker tool package. For comparison, the polarizable continuum model (PCM)[49] was used to simulate interaction of valerophenone and its one-water complex with the water environment.

Results and Discussion

Structures and Relative Energies. After 15 ns MD simulations, a few snapshots were chosen as the starting geometries (Scheme 1) for the iterative QM and MM optimizations of the S_0, $^3n\pi^*$, $^3\pi\pi^*$, $^1n\pi^*(S_1)$, and $^1\pi\pi^*(S_2)$ structures. The CAS(10,9)/6-31G* optimized structures for the VP−H_2O complex in the five electronic states are schematically shown in Figure 1 along with the selected bond parameters. The most stable structure for the one-water complex in the S_0 state, VP−H_2O−S_0, has no symmetry with the C7−C8−C9−C10 dihedral angle of −73.9°. In the ground state, the aromatic ring is almost a regular hexagon with the C−C−C angle in the range of 118.9−120.5° and the largest difference of 0.012 Å in the C−C bond length. The iterative CAS(10,9)/6-31G* and MM (Amber) optimizations reveal that effects from the bulk surrounding water have little influence on

(45) Zhang, Y.; Liu, H.; Yang, W. *J. Chem. Phys.* **2000**, *112*, 3483–3492.
(46) Li, J.; Ai, Y.-J.; Xie, Z.-Z.; Fang, W.-H. *J. Phys. Chem. B* **2008**, *112*, 8715–8723.
(47) Frisch, M. J. et al. *Gaussian 03*, revision B.02; Gaussian, Inc.: Pittsburgh PA, 2003.
(48) MOLPRO is a package of ab initio programs written by Werner, H.-J. and Knowles, P. J. with contributions from Amos, R. D. et al.
(49) Cossi, M.; Barone, V.; Robb, M. A. *J. Chem. Phys.* **1999**, *111*, 5295.

SCHEME 1. Model System for Aqueous Valerophenone, Along with the Atom-Labeling Scheme Illustrated in the QM Structure

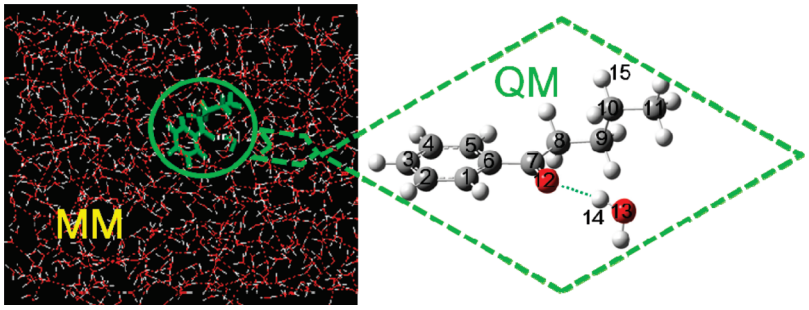

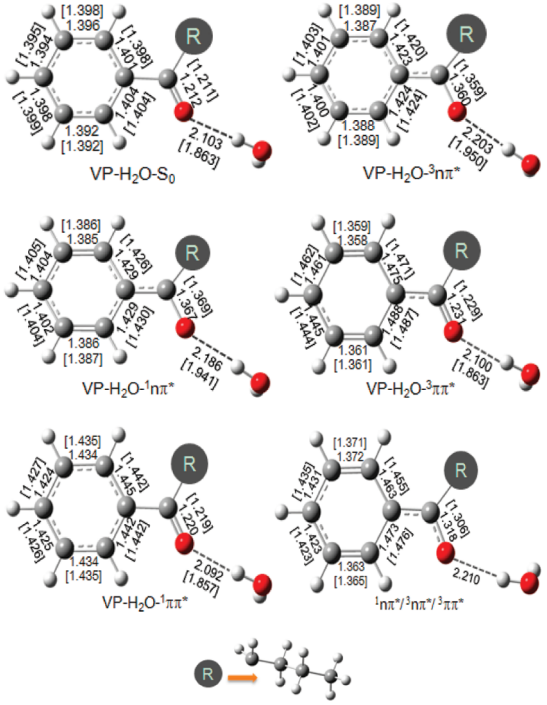

FIGURE 1. Schematically stationary structures for the VP−H_2O complex in the lowest five electronic states, along with the selected bond parameters (bond lengths in angstroms and bond angles in degrees). The parameters in square brackets come from iterative CAS(10,9)/6-31G* and Amber field optimizations of the complex in the water box. The three-surface intersection structure is shown with the bond parameters of free valerophenone given in square brackets.

bond parameters of the VP molecule. However, the intermolecular H-bond distance (H14···O12) is decreased from 2.103 Å in the isolated one-water complex to 1.863 Å in aqueous solution. It is evident that the intermolecular H-bond is significantly strengthened due to the interaction between the complex and the solvent H_2O molecules. It should be pointed out that the remarkable effect of the bulk water surrounding on the intermolecular H-bond was not observed by the CAS(10,9)/6-31G* calculations with the PCM model, which predict the H14···O12 distance to be 2.107 Å for the VP−H_2O−S_0 complex in aqueous solution. As shown in Scheme 1, where the atom numbering is given for the QM moiety, there is a large H-bond network in the bulk water surrounding. More importantly, there exist the strong Coulomb interactions between the solute and solvent molecules. These are main reasons why the polarizable continuum model (PCM) cannot provide a good description

SCHEME 2

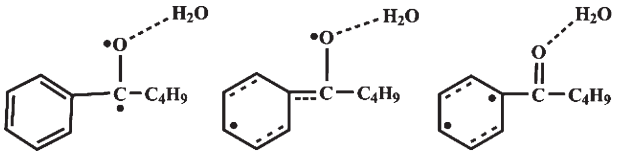

on the intermolecular interaction for the complex in aqueous solution.

Upon electronic excitation to the S_1 state, the most striking change in structure is associated with the C7−O12 bond length, which is 1.212 Å in VP−H_2O−S_0 and becomes 1.367 Å in the S_1 structure of the VP−H_2O complex (VP−H_2O−S_1). The CAS(10,9) calculated wave functions show that the S_1 state is of $^1n\pi^*$ character. It is easy to understand that the n→π^* electronic transition reduces the π-bonding character of the carbonyl group, thus the C7−O12 distance is increased significantly. The H14···O12 distance is predicted to be 2.186 Å in the VP−H_2O−$^1n\pi^*$ structure, which is 0.083 Å longer than the corresponding value in the S_0 structure. As shown in Figure 1, the structure of the VP−H_2O complex in the $^3n\pi^*$ state (VP−H_2O−$^3n\pi^*$) is very similar to that of the complex in the $^1n\pi^*$ state.

The intermolecular H-bond in the complex is significantly weakened due to an excitation to the $^1n\pi^*$ or $^3n\pi^*$ state. From a general understanding of hydrogen-bond interaction,[50] the O12···H14 hydrogen bond in the complex originates mainly from a donation of the lone-pair electrons of the O12 atom to the H14−O13 σ^* orbital. One of the lone-pair electrons is excited to the C=O π^* orbital in the n,π^* states, which leads to a decrease of the electron density on the O12 atom. As a result, the O12···H14 hydrogen bond is significantly weakened in the $^3n\pi^*$ and $^1n\pi^*$ states, as compared with that in the S_0 state. Unlike an electronic excitation, the intermolecular H-bond interaction in the $^3n\pi^*$ or $^1n\pi^*$ complex is strengthened by the solvent effect from the bulk surrounding H_2O molecules, which is similar to that in the ground state.

As shown in Scheme 2, the $^3n\pi^*$ and $^1n\pi^*$ electronic states are of similar biradical character, which is mainly localized in the carbonyl group. Therefore, the n→π^* electronic transition only has a little influence on the structure of the aromatic ring. However, the structure of the aromatic ring is remarkably changed by the π→π^* electronic transition. In the $^3\pi\pi^*$ state, the C1−C2 and C4−C5 bond distances are

(50) Kollman, P. A.; Allen, L. C. *Chem. Rev.* **1972**, *72*, 283–303.

TABLE 1. Calculated Adiabatic Excitation Energies (kcal/mol), Dipole Moments (Debye, in parentheses), and Oscillator Strength (*f*)

	VP	VP−H_2O			
	CAS	CAS	CAS/Amber	CASPT2//CAS/Amber	$f(S_0 \rightarrow T_n, S_n)$
S_0	0.0	0.0	0.0	0.0(6.4)	−
$^3n\pi^*$	75.1	77.1	77.3	78.2(4.4)	9.2×10^{-6}
$^3\pi\pi^*$	75.5	75.5	74.2	76.5(7.2)	1.4×10^{-4}
$^1n\pi^*$	78.7	80.2	80.4	83.2(4.3)	6.9×10^{-5}
$^1\pi\pi$	105.9	105.6	104.3	98.8(8.0)	0.47

about ~1.36 Å, and the two bonds are mainly of double-bond character. The other C−C bond distances in the aromatic ring exhibit clear C−C single bond nature. The geometric features of the $^3\pi\pi^*$ state are consistent with its electronic structure plotted in Scheme 2. The electronic and geometric structures of the $^1\pi\pi^*(S_2)$ state are quite different from those for the $^3\pi\pi^*$ state. Two unpaired electrons are delocalized into the whole aromatic ring, which results in an uniform increase of the ring C−C bonds to ~1.43 Å in the S_2 state. However, the $\pi \rightarrow \pi^*$ transition has a little influence on structure and nature of the carbonyl group. As a result, the intermolecular H-bond structure of the $^3\pi\pi^*$ or $^1\pi\pi^*$ complex is close to that for the complex in the S_0 state, but different from that in the $^3n\pi^*$ or $^1n\pi^*$ complex.

The adiabatic excitation energies to the $^3n\pi^*$, $^3\pi\pi^*$, $^1n\pi^*$, and $^1\pi\pi^*$ states were calculated at different levels for VP and VP−H_2O in the gas phase and aqueous solution, which are given in Supporting Information. Table 1 lists the CAS(10,9), CAS(10,9)/Amber, and CASPT2//CAS(10,9)/Amber calculated adiabatic excitation energies for valerophenone and its one-water complex. The first observation is that the interaction between the solvent and the solute has an important effect on the relative energies of the $n\pi^*$ and $\pi\pi^*$ excited states. The adiabatic excitation energies to the $^3n\pi^*$ and $^3\pi\pi^*$ states are 75.1 and 75.5 kcal·mol^{-1}, respectively, for the free valerophenone molecule at the CAS(10,9) level. However, formation of the one-water complex results in inversion of the $^3n\pi^*$ and $^3\pi\pi^*$ relative energies, which are, respectively, 77.1 and 75.5 kcal·mol^{-1} in the isolated VP−H_2O complex. A comparison with the CAS(10,9)/Amber calculated result shows that the $^3n\pi^*$ relative energy is little influenced by the interaction between the complex and the bulk surrounding water. The $^3\pi\pi^*$ state is confirmed to be the lowest triplet state by the CASPT2//CAS(10,9)/Amber calculations for the VP−H_2O complex in aqueous solution, and the energy difference between the $^3n\pi^*$ and $^3\pi\pi^*$ states is 1.7 kcal·mol^{-1}. The $^1n\pi^*$ state is increased by about 2.0 kcal·mol^{-1} in energy, due to the intermolecular hydrogen bonding in the VP−H_2O complex, while the relative energy of the $^1n\pi^*$ state is nearly unchanged by the solvent effect from the bulk surrounding water. On the contrary, the $^1\pi\pi^*$ state is significantly lowered in energy by the bulk solvent effect, and formation of the VP−H_2O complex has little influence on the relative energy of the $^1\pi\pi^*$ state.

The UV absorption spectra of valerophenone were measured in different solvents with wide spectral region (200−315 nm).[34] The absorption maximum was located at 237 nm for valerophenone in nonpolar hexane (n-C_6H_{14}) solvent, which corresponds to the $\pi \rightarrow \pi^*$ transition. The absorption maximum is red-shifted to 245 nm for aqueous valerophenone. In addition, a blue shift was observed for the weak $n \rightarrow \pi^*$ transition in the UV-B region (280−315 nm).[34] A comparison of the calculated results in Table 1 reveals that the blue shift of the $n \rightarrow \pi^*$ transition arises mainly from the hydrogen-bonding effect from the explicit water in the complex. As pointed out before, the intermolecular H-bond in the one-water complex is weakened due to the $n \rightarrow \pi^*$ electronic excitation. In other words, the ground-state complex is stabilized more than the complex in the n,π^* excited states by the H-bonding interaction, which is mainly responsible for the blue shift of $n \rightarrow \pi^*$ transition observed in the absorption spectrum of aqueous valerophenone.

In the ground state, the π electrons are uniformly distributed in the aromatic ring of the VP molecule. However, positive and negative charge centers are a little separated, due to one π electron excited to the π^* orbital. The vertical excitation from S_0 to Franck−Condon structure of the $^1\pi\pi^*$ state results in dipole moment increase from 6.2 to 9.4 D, which are calculated at the CASPT2//CAS/Amber level. As listed in Table 1, the $^1\pi\pi^*$ equilibrium structure has a dipole moment of 8.0 D, larger than that in the ground state. The calculated adiabatic excitation energies reveal that the red shift of the $\pi \rightarrow \pi^*$ transition observed in the absorption spectrum of aqueous valerophenone originates from the effect of the bulk surrounding water. Since the effect of the bulk surrounding water mainly comes from the Coulomb interactions, the $^1\pi\pi^*$ state that has relative large dipole moment is decreased more in energy than the S_0 state. Therefore, the red-shifted transition observed in the absorption spectrum should be attributed to a large increase in dipole moment accompanying the $\pi \rightarrow \pi^*$ transition. This is consistent with the experimental observation that the red shift is gradually changed from nonpolar hexane (~237 nm) to polar acetonitrile (239 nm) and to water (245 nm).[34]

The $^1n\pi^*/^3n\pi^*/^3\pi\pi^*$ Three-Surface Intersection. It has been well-established that aromatic ketones have some unique photochemical and photophysical features, such as a short singlet lifetime, high phosphorescence, and weak fluorescence. These features clearly show that intersystem crossing (ISC) to the triplet state is very efficient in aromatic carbonyl compounds upon photoexcitation to an excited singlet state. To explore the underlying reason for the efficient ISC process, we tried to search for the minimum energy crossing point between the $^1n\pi^*$ and $^3\pi\pi^*$ states as well as between the $^3n\pi^*$ and $^3\pi\pi^*$ states. The detailed structures and energies for the intersections are available in the Supporting Information. The singlet and triplet surface crossing was determined by use of Slater determinants in the state-averaged CASSCF calculations and was identified as the $^1n\pi^*$ and $^3\pi\pi^*$ surface crossing ($^1n\pi^*/^3\pi\pi^*$). Similarly, the intersection between the two triplet surfaces was determined as one between the $^3\pi\pi^*$ and $^3n\pi^*$ surfaces ($^3\pi\pi^*/^3n\pi^*$). The optimized structures show that $^1n\pi^*/^3\pi\pi^*$ and $^3\pi\pi^*/^3n\pi^*$ are indistinguishable from one another in structure, and the two crossing points have the same energy. In fact, the $^1n\pi^*$, $^3\pi\pi^*$, and $^3n\pi^*$ states intersect in the same region ($^1n\pi^*/^3\pi\pi^*/^3n\pi^*$) for the one-water complex. An analogous three-surface intersection was found for free valerophenone. As shown in Figure 1, the $^1n\pi^*/^3\pi\pi^*/^3n\pi^*$ structure is less influenced by formation of the one-water complex, except for the C7−O12 distance that is elongated by 0.012 Å from free valerophenone to the complex.

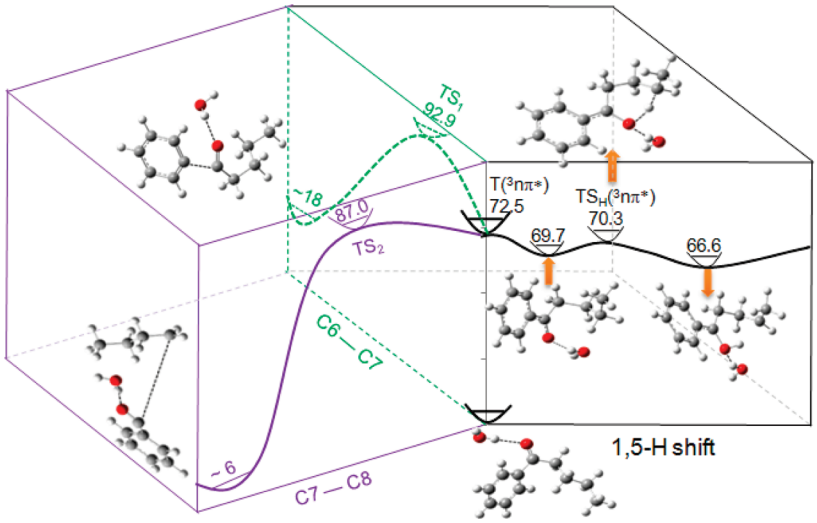

FIGURE 2. Potential energy surfaces of the α-C−C cleavages and 1,5-H shift reactions starting from the $^3n\pi^*$ state, along with the UB3LYP/6-311G**/Amber calculated relative energies for the stationary structures (kcal·mol^{-1}).

In the $^1n\pi^*$ or $^3n\pi^*$ structure, two unpaired electrons are mainly distributed in the carbonyl C7 and O12 atoms, respectively, while the two singly occupied electrons are populated in the aromatic ring in the $^3\pi\pi^*$ structure. As shown in Scheme 2, the $^1n\pi^*/^3\pi\pi^*/^3n\pi^*$ electronic structure is located between $^1n\pi^*(^3n\pi^*)$ and $^3\pi\pi^*$ with the two unpaired electrons distributed in the O12 atom and the aromatic ring, respectively. The differences in the S_1 and $^1n\pi^*/^3\pi\pi^*/^3n\pi^*$ structures mainly result from the redistribution of the conjugation π electrons and thus would not be expected to give rise to a substantial change in the energy. The $^1n\pi^*/^3\pi\pi^*/^3n\pi^*$ structure is 2.2 kcal·mol^{-1} above the S_1 minimum. It is reasonable to expect that the investigated system relaxes to the $^1n\pi^*/^3\pi\pi^*/^3n\pi^*$ intersection point very easily after photoexcitation to the S_1 state. As discussed in the previous studies,[42] there is no first-order spin−orbit coupling for the $^1n\pi^*\rightarrow{}^3n\pi^*$ transition, and the direct $^1n\pi^*\rightarrow{}^3n\pi^*$ intersystem crossing takes place with low efficiency. However, the $^3\pi\pi^*$ state acts as a relay and enables the $^1n\pi^*\rightarrow{}^3n\pi^*$ ISC to occur with high efficiency, due to the existence of the $^1n\pi^*/^3\pi\pi^*/^3n\pi^*$ intersection. The $^1n\pi^*/^3\pi\pi^*/^3n\pi^*$ intersection holds the key to understanding much of the relaxation dynamics of the S_1 state.

Norrish Type I and II Reactions. Both Norrish type I and II reactions proceed along the triplet state pathway, which has been observed for most aromatic ketones.[28−34] Here we performed iterative UB3LYP/6-311G** and MM (Amber force field) optimizations of the stationary structures for the α-C−C bond cleavage and the 1,5-H shift reactions starting from the $^3n\pi^*$ state. The obtained bond parameters and energies are given in Supporting Information. Potential energy surfaces of the α-C−C cleavages and 1,5-H shift reactions are shown in Figure 2, along with the relative energies of the stationary structures at the UB3LYP/6-311G**/Amber level. In the ground state, the most stable isomer for valerophenone in the gas phase and aqueous solution has an all-trans-form structure for the C_4H_7 alkyl chain. However, the most stable isomer in the $^3n\pi^*$ state for VP−H_2O in water solution has a structure favorable for the 1,5-H shift reaction, and the all-trans-form structure becomes the second stable isomer in the $^3n\pi^*$ state, which is 2.8 kcal·mol^{-1} higher than the most stable isomer.

Two transition states on the triplet pathway were determined for the α-C6−C7 and α-C7−C8 cleavages of the VP−H_2O complex, labeled TS_1 and TS_2, respectively, hereafter. The aromatic ring and the carbonyl group are nearly coplanar in the $^3n\pi^*$ structure, due to their conjugation interaction, but the aromatic ring and the carbonyl group are almost perpendicular to each other in the TS_1 structure. The C6−C7 distance is significantly increased from 1.432 Å in the $^3n\pi^*$ state to 2.166 Å in the TS_1 structure. As a result, the conjugation interaction disappears in the TS_1 structure, and the acyl group can rotate with respect to the aromatic ring. The barrier height was predicted to be 14.9 kcal·mol^{-1} for the α-C7−C8 cleavage of the VP−H_2O complex, which is 12.1 kcal·mol^{-1} lower than that for the α-C6−C7 cleavage. To include the effect of the bulk surrounding water, the TS_1 and TS_2 structures were reoptimized for the VP−H_2O complex in the water box using the combined UB3LYP/6-311G** and MM (Amber force field) method. The most striking change is associated with the barrier height of the α-C6−C7 cleavage, which is reduced from 27 kcal·mol^{-1} for free VP−H_2O complex to the 20.4 kcal·mol^{-1} for the complex in aqueous solution. In addition, the barrier of the α-C7−C8 cleavage is decreased by 0.5 kcal·mol^{-1} due to the effect of the bulk surrounding water.

The transition state of the 1,5-H shift from the $^3n\pi^*$ state has been optimized at the UB3LYP/6-311G** level of theory for valerophenone and its one-water complex and confirmed to be the first-order saddle point on the lowest triplet surface, referred to as TS_H hereafter. The 1,5-H shift has a barrier of 4.6 kcal·mol^{-1} for free valerophenone, and it becomes 3.8 kcal·mol^{-1} for the one-water complex (VP−H_2O). Formation of the complex has little influence on the 1,5-H shift reaction. However, the barreir to the 1,5-H shift is significantly reduced by the bulk surrounding water. The combined UB3LYP/6-311G** and MM (Amber force field) calculations reveal that the 1,5-H shift has a barrier of 0.6 kcal·mol^{-1} for the complex in water solution, which is much lower than those for the α-C−C cleavages. As discussed before, the

most stable isomer is the all-trans structure in the ground state, while in the $^3n\pi^*$ state, the all-trans structure is about 2.8 kcal·mol^{-1} higher than the most stable isomer that has a favorable conformer for the 1,5-H shift. There is a very small barrier on the isomerization pathway from the all-trans structure to the favorable conformer for the 1,5-H shift. Thus, the isomerization followed by the 1,5-H shift is a predominant channel in the lowest triplet state, and the α-C−C cleavages are not in competition with the 1,5-H shift reaction. This is consistent with the experimental findings that Norrish type II quantum yield is close to unity throughout the 290−330 nm spectral region.[34]

On the basis of quenching studies with steady-state irradiations, the triplet lifetime of valerophenone in aqueous solution was estimated to be 52 ns, ~7 times longer than that observed in hydrocarbon solvents.[34] The present calculations show that there is a very small barrier on the triplet-state pathway, and the 1,5-H shift is an ultrafast process, which seems to be contrary to long triplet lifetime of valerophenone in aqueous solution. Since the $^1n\pi^*/^3\pi\pi^*/^3n\pi^*$ three-surface intersection exists for valerophenone, both $^3\pi\pi^*$ and $^3n\pi^*$ states can be populated upon photoexcitation to the $^1n\pi^*$ state in the wavelength range of 290−330 nm. The $^3n\pi^*$ state is the lowest triplet state for valerophenone in the gas phase (in hydrocarbon solvent), but the $^3\pi\pi^*$ state is lower than the $^3n\pi^*$ state in energy for valerophenone in aqueous solution. As shown in Scheme 2, the n→π* excitation is localized in the carbonyl group and the $^3n\pi^*$ state exhibits radical-like reactivity, while the π→π* excitation is localized in the aromatic ring and the $^3\pi\pi^*$ state is unreactive in view of the 1,5-H shift. The lowest triplet-state character switches from the reactive n,π* to unreactive π,π* for valerophenone in aqueous solution, and the $^3\pi\pi^*$ state is responsible for the long triplet lifetime of aqueous valerophenone. It is evident that the 1,5-H shift from the $^3n\pi^*$ state was predicted to proceed very fast by the present calculation, which is not inconsistent with the long triplet ($^3\pi\pi^*$) lifetime observed experimentally.

Summary

In the present work, we report the first theoretical study on the excited-state nature and Norrish type reactions for valerophenone in aqueous solution, using the combined molecular mechanics and high-level ab initio methods. Structures and relative energies of the lowest five electronic states were determined for valerophenone in the gas phase (in hydrocarbon solvents) and aqueous solution. The n→π* and π→π* excitations were found to localize on the carbonyl group and the aromatic ring, respectively, which gives evidence that the $^3n\pi^*$ state is reactive and the $^3\pi\pi^*$ state is unreactive in view of the 1,5-H shift. Formation of the intermolecular hydrogen bond in the complex of valerophenone with water results in a blue shift of the n,π* excited states, while the Coulomb interaction between valerophenone and the bulk surrounding water is mainly responsible for the red shift of the π,π* excited states. As a result, the lowest triplet state of valerophenone is switched from $^3n\pi^*$ in hydrocarbon solvents to $^3\pi\pi^*$ in aqueous solution. Probably, the long triplet lifetime observed for aqueous valerophenone originates from the $^3\pi\pi^*$ state.

The $^1n\pi^*$, $^3\pi\pi^*$, and $^3n\pi^*$ states were found to intersect in the same structural region for valerophenone and its one-water complex. The structural similarity and very small energy differences between the $^1n\pi^*$ minimum and the three-surface $^1n\pi^*/^3\pi\pi^*/^3n\pi^*$ intersection give us reason to expect that the system relaxes to the $^1n\pi^*/^3\pi\pi^*/^3n\pi^*$ intersection very easily after photoexcitation to the S_1 state. Because of the existence of the $^1n\pi^*/^3\pi\pi^*/^3n\pi^*$ intersection, the $^3\pi\pi^*$ state acts as a relay and enables the $^1n\pi^*\rightarrow{}^3n\pi^*$ ISC to occur with high efficiency. This appears to be the main reason why the intersystem crossing (ISC) from $^1n\pi^*$ to $^3n\pi^*$ is very efficient for aqueous valerophenone, and most of aromatic ketones have unique photophysical features such as a short singlet lifetime, high phosphorescence, and weak fluorescence.

As a result of very efficient ISC to the triplet state, both Norrish type I and II reactions proceed from the $^3n\pi^*$ state for aqueous valerophenone. The Coulomb interaction between valerophenone and the bulk surrounding water has a significant influence on the α-C−C cleavage and the 1,5-H shift reaction, but the most striking change is associated with the barrier height of the α-C6−C7 cleavage, which is reduced from 27 kcal·mol^{-1} for free VP−H_2O complex to the 20.4 kcal·mol^{-1} for the complex in aqueous solution. However, the 1,5-H shift is predicted to have a very small barrier on the triplet pathway, and the α-C−C bond cleavages are not in competition with the 1,5-H shift reaction. This is in good agreement the experimental findings that Norrish type II quantum yield is close to unity upon photoexcitation of aqueous valerophenone in the wavelength region of 290−330 nm.

The triplet lifetime of aqueous valerophenone was estimated to be 52 ns, ~7 times longer than that observed in hydrocarbon solvents,[34] which seems to be contrary to very fast 1,5-H shift process for valerophenone in aqueous solution. As pointed out before, the $^3n\pi^*$ state is the lowest triplet state for valerophenone in the gas phase (in hydrocarbon solvent), but the $^3\pi\pi^*$ state is lower than the $^3n\pi^*$ state in energy for valerophenone in aqueous solution. As a result, relative populations of the $^3n\pi^*$ state are significantly reduced for valerophenone in aqueous solution, as compared with those in hydrocarbon solvent. The $^3\pi\pi^*$ state is responsible for the long lifetime of aqueous valerophenone. Thus, the 1,5-H shift from the $^3n\pi^*$ state that proceeds very fast is not inconsistent with the long triplet lifetime observed experimentally.

Acknowledgment. This work was supported by grants from the NSFC (Grant No. 20720102038) and from the Major State Basic Research Development Programs (Grant No. 2004CB719903).

Supporting Information Available: Cartesian coordinates and absolute energies of the stationary and intersection structures are available. This material is available free of charge via the Internet at http://pubs.acs.org.